DANISH METEOROLOGICAL INSTITUTE

——— SCIENTIFIC REPORT ———

01-06

Impact of ATOVS AMSU-A radiance data in the DMI-HIRLAM 3D-Var analysis and forecasting system

Bjarne Amstrup

COPENHAGEN 2001

ISSN Nr. 0905-3263 (printed)
ISSN Nr. 1399-1949 (online)
ISBN-Nr. 87-7478-443-9

Impact of ATOVS AMSU-A radiance data in the DMI-HIRLAM 3D-Var analysis and forecasting system

Bjarne Amstrup
Danish Meteorological Institute

Abstract

This report describes the preliminary results from an observing system experiment (OSE) using Advanced TIROS (Television Infra-Red Observation Satellite) Operational Vertical Sounder (ATOVS) brightness temperatures from the polar orbiting satellite NOAA16 (National Oceanic and Atmospheric Administration) in near real-time in a period from late June to the end of September 2001. All AMSU-A (Advanced Microwave Sounding Unit-A) level 1c data (channels 1 to 10, only) available from locally received data from the DMI Smidsbjerg antenna as well as from the DMI Sdr. Strømfjord/Kangerlussuaq (Greenland) antenna have been used.

A new observation error covariance matrix has been calculated using data from a two month period with passive inclusion of NOAA16 data received via the DMI Smidsbjerg antenna. Subsequently a second observation error covariance matrix was calculated using data from a later one month period including data from the DMI Sdr. Strømfjord antenna.

Based on observation (obs-) and field verification the impact is basically neutral in this period. There is a marginal positive impact on some parameters based on obs-verification.

1. Introduction

(A)TOVS data have been assimilated at ECMWF (European Centre for Medium-Range Weather Forecasts), NCEP (National Centre for Environmental Prediction), Météo France, UKMO (United Kingdom Meteorological Office) for a number of years and are considered to be the most important non-conventional data of the observing system (see, e.g., Bouttier and Kelly, 2001). The (A)TOVS-related research and development activities within the HIRLAM (HIgh Resolution Limited Area Model) project also have a long history, dating back to Gustafsson and Svensson, 1988. However, no HIRLAM operational system contains ATOVS data assimilation.

Recently, an intense effort has been made to include the ATOVS in the HIRLAM variational data assimilation system (HIRVDA). Data assimilation experiments have been made at SMHI (Swedish Meteorological and Hydrological Institute) and DNMI (Det norske meteorologiske institutt). The results have so far been mixed, but recently a new impact study at DNMI (Tveter and Vignes, 2001) has shown a positive impact. This result is, however, based on a very short period and very limited data coverage and data from the NOAA15 polar orbiting satellite. The present impact study is based on data from the newer NOAA16 satellite that are free of the problem with the Advanced Very High Resolution Radiometer (AVHRR) radiometer instrument as do NOAA15. Besides being an OSE (Observation System Experiment) it is a step in the pre-operational testing of ATOVS at DMI by:

1) making necessary statistics such as the first bias correction file and observation error covariance matrix and

2) testing the stability of the DMI-HIRLAM 3D-Var (three dimensional variational) analysis system including these data.

Section 2 describes briefly the ATOVS AMSU-A instrument and the usage of ATOVS AMSU-A brightness temperatures in the HIRLAM 3D-Var system as well as some results from passive inclusion of the data prior to and during the real experiment. Section 3 describes the DMI-HIRLAM 3D-Var analysis system and forecasting system as well as some changes made during the runs. Section 4 gives some results, and finally a summary of the conclusions drawn from the experiments is given in section 5.

2. The ATOVS instruments and ATOVS AMSU-A usage in HIRLAM 3D-Var

The two most recent polar orbiting satellites in the National Oceanic and Atmospheric Administration (NOAA) series, NOAA15 and NOAA16, are carrying a new generation of instruments on board called ATOVS. The ATOVS instruments are: AMSU-A1/AMSU-A2 (Advanced Microwave Sounding Unit-A), AMSU-B (Advanced Microwave Sounding Unit-B), HIRS/3 (High Resolution Infrared Radiation Sounder/3), and AVHRR/3 (Advanced Very High Resolution Radiometer/3). The instruments provide passive measurements of the radiation emitted from the earth's surface and throughout the atmosphere. The radiances contain temperature as well as humidity information. The AMSU-A instruments used so far in HIRLAM 3D-Var have 15 channels in total of which 4 (channels 1, 2, 3 and 15) measure in “window” spectral regions and the remaining 11 channels are “temperature sounding” channels. The temperature sounding channels can be used to derive atmospheric temperature profiles from the surface to an altitude of about 40 km. However, areas with precipitation can cause erroneous estimates of the temperature in the lower troposphere and measurements in such areas should not be used without extra precautions, if used at all. The window channels receive energy primarily from the surface and the boundary layer, and can be used, for example, to derive total precipitable water and cloud liquid water. See `http://www2.ncdc.noaa.gov/docs/klm/` for further details on the NOAA15 and NOAA16 instruments, and `http://www.ecmwf.int/services/dcover/index_rad.html` for ECMWF usage of HIRS and AMSU radiance data and monitoring of the data.

The data used in the present impact study are data received locally from the Smidsbjerg and Sdr. Strømfjord (Kangerlussuaq) antennas and further processed with the AAPP (ATOVS and AVHRR Processing Package) package (see `http://www.eumetsat.`

Table 1: Observation error covariance matrix (for channels 1 to 10) used in part of the current (from 2001071900 to 2001082118) ATOVS HIRLAM 3D-Var impact experiment. The unit is kelvin squared. The matrix is based on data for March and April 2001, with a global scaling factor of $\gamma = 0.30$. Note that the matrix is symmetric.

5.139	4.536	2.793	0.636	0.088	0.030	0.019	0.027	0.022	0.014
4.536	**6.671**	4.457	0.817	0.140	−0.129	−0.052	−0.020	−0.181	−0.365
2.793	4.457	**8.804**	1.349	0.317	−0.601	−0.203	−0.209	−0.714	−1.652
0.636	0.817	1.349	**0.392**	0.094	−0.065	−0.057	−0.029	−0.064	−0.158
0.088	0.140	0.317	0.094	**0.042**	−0.017	−0.014	−0.007	−0.025	−0.054
0.030	−0.129	−0.601	−0.065	−0.017	**0.099**	0.042	0.038	0.107	0.209
0.019	−0.052	−0.203	−0.057	−0.014	0.042	**0.053**	0.030	0.035	0.046
0.027	−0.020	−0.209	−0.029	−0.007	0.038	0.030	**0.039**	0.047	0.077
0.022	−0.181	−0.714	−0.064	−0.025	0.107	0.035	0.047	**0.162**	0.300
0.014	−0.365	−1.652	−0.158	−0.054	0.209	0.046	0.077	0.300	**0.668**

Table 2: Observation error covariance matrix (equivalent to Table 1) based on a month of data from July 20 to August 21, 2001, with a global scaling factor of $\gamma = 0.30$.

6.624	5.383	4.290	0.860	0.091	−0.050	0.034	0.034	−0.035	−0.087
5.383	**8.242**	6.264	1.051	0.177	−0.143	0.033	0.051	−0.122	−0.236
4.290	6.264	**11.675**	1.872	0.505	−0.479	0.074	0.077	−0.204	−0.682
0.860	1.051	1.872	**0.529**	0.129	−0.079	−0.026	0.001	−0.027	−0.089
0.091	0.177	0.505	0.129	**0.057**	−0.026	−0.006	0.003	−0.014	−0.036
−0.050	−0.143	−0.479	−0.079	−0.026	**0.060**	0.017	0.009	0.035	0.064
0.034	0.033	0.074	−0.026	−0.006	0.017	**0.049**	0.025	0.013	−0.002
0.034	0.051	0.077	0.001	0.003	0.009	0.025	**0.033**	0.011	0.002
−0.035	−0.122	−0.204	−0.027	−0.014	0.035	0.013	0.011	**0.047**	0.055
−0.087	−0.236	−0.682	−0.089	−0.036	0.064	−0.002	0.002	0.055	**0.125**

`de/en/index.html`): The raw (level 0) data received are processed in 3 steps to level 1c (geo-referenced and calibrated temperatures and albedo) data. The resulting level 1c data containing brightness temperatures for the 15 AMSU-A channels are then further processed separately from AAPP to the standard BUFR-format (WMO, 1995). The data from Sdr. Strømfjord have been available since late May 2001. By receiving the data this way they can easily be made available for assimilation within one hour of the observation time.

Before being used in the data assimilation, the AMSU-A data from NOAA16 have been included passively in 3D-Var for more than 2 months to accumulate the necessary statistics needed for assimilation. Here passive mode means that the ATOVS data are processed and the innovations (observation−background, see later) computed but not used in further analysis steps. The data used for this step were data received locally from the Smidsbjerg antenna only since data from Sdr. Strømfjord have been available only since late May 2001. Bias- and rms-statistics from the passive inclusion runs for the AMSU-A data available on a daily basis for the 15 channels are shown in Figure 1. The statistics involve a somewhat varying number of data day by day since not all NOAA16 passages have been received, other satellites having higher priorities. The results indicate that the "surface"-channels 1-3 have rather high rms-values and are of little value in assimilation, and also that channels 11 to 15 have high bias- and rms-values when compared with derived results from the first guess fields and should not be considered for assimilation. The main reason for not using channels 11 to 15 is that the response functions/weight functions (shown in Figure 2) for these channels have significant amplitudes over the vertical limit of the DMI-HIRLAM models, 10 hPa. If they are to be used at a later time either the vertical limit of the DMI-HIRLAM model should be extended upwards or ECMWF forecasts should be used for data above 10 hPa instead of the climate values used presently above 10 hPa. Channel 10 also has a tail part above 10 hPa. However, the use of the different channels is determined by the ATOVS observation error covariance matrix. For the first 3 weeks (up to 2001071900) in the present data impact study an error covariance matrix from SMHI with only diagonal elements was used and a value of 900 was used for channels 1-4 and 11-15. A new observation error covariance matrix was designed using a global scaling factor of $\gamma = 0.30$ as described in Tveter and Vignes, 2001:

$$\mathbf{R} = \gamma \langle (\mathbf{y} - \mathbf{H} \cdot \mathbf{x}_a) \cdot (\mathbf{y} - \mathbf{H} \cdot \mathbf{x}_a)^T \rangle \,. \tag{1}$$

In (1) $\langle \ldots \rangle$ denotes the average value, $\mathbf{y}$ is an ATOVS observation vector, $\mathbf{H}$ is the forward model, and $\mathbf{x}_a$ is the analysis that resulted from using all standard types of observations *except* ATOVS. However, for the present calculations the first guess (or background) fields have been used instead of the analysis fields. The first guess fields are 3 h forecasts from the precedent data assimilation cycle. A new series using analysis fields for this purpose was started September 1. For the first 10 days only small differences are observed for a matrix calculated from the differences between analyses and a matrix calculated from the differences with first guesses. The two month period March and April was used and the result for channels 1-10 is given in Table 1. The corresponding result for a one month period in July and August is shown in Table 2. The one month period has been calculated from a passive inclusion of all available data from both local antennas in the parallel run. Note that the matrices are symmetric. The forward model $\mathbf{H}$ is an important part in the 3D-Var analysis system. Given a model state it calculates the model equivalent of the observed quantity at the position of the observation. The radiative forward model presently used for calculating brightness temperatures is based on RTTOV-5 (Radiative Transfer model for TOVS, release 5), available from from the Numerical Weather Prediction SAF (Satellite Application Facility) (see `http://www.metoffice.com/sec5/NWP/NWPSAF/index.html` and Saunders *et al.*, 1999). RTTOV-6 has been released but it has been considered more important, e.g., to include a first guess check of the brightness temperatures than to update the radiation transfer model in the HIRLAM 3D-Var analysis system.

As an example of the data coverage, the data available on September 8, 2001 is shown in Figure 3. The coverage of the Atlantic north of 40° is very good. At present, however, only brightness temperatures over sea are used—data over land and over ice are not used.

3. HIRLAM 3D-Var data assimilation system

The operational data assimilation system for DMI-HIRLAM-G has since the end of September 2000 been a 3D-Var analysis scheme (version 4.2) (Gustafsson *et al.*, 1999; Gustafsson *et al.*, 2001; Lindskog *et al.*, 2001) and a forecast model (version 4.5 with some updates). The DMI system is documented in Sass *et al.* (2000) and Mogensen *et al.* (2000).

The version used here is the HIRLAM 3D-Var 4.4.1 OpenMP version for NEC. The main difference relative to the operational HIRLAM 3D-Var version is that PILOT data originating from a station with radiosonde data are screened if a TEMP is available at the same time.

The observation window covers a 3 h span around the analysis time (00, 03, 06, 09, 12, 15, 18 and 21 UTC) except for a 6 h span around the analysis times 06 UTC and 18 UTC before the long forecasts starting from these. For AMDAR/ACARS (Aircraft Meteorological Data Reporting/Aircraft Communication Addressing and Reporting System) aircraft observation data a $\pm\frac{1}{2}$ h observation time window is used to reduce along track analysis increments leading to spurious effects in the following forecast. A standard observation set is used, including synoptic observations, ship observations, (drifting and moored) buoys, pilot balloons, radiosonde data and aircraft data. The run with these observation types is denoted NOA (NO ATOVS) and the run denoted WIA (WIth ATOVS) also uses NOAA16 AMSU-A brightness temperature data as described in the previous section. The first guess field is a 3 h forecast from the precedent data assimilation cycle except for a 6 h forecast for the analyses at 06 UTC and 18 UTC before the long forecasts starting from these.

The basic model applied in the present parallel experiment is DMI-HIRLAM-G (see Sass *et al.*, (2000) for details), based on HIRLAM reference version 4.5/4.6. The horizontal resolution is 0.45°, the number of vertical levels 31, the number of grid points is 190×202, the time step is 240 s and the lateral boundary values are updated every 6 hours from ECMWF forecasts.

Twice a day (at 00 UTC and 12 UTC reassimilation cycles) the DMI-HIRLAM-G model is restarted from fresh ECMWF analyses using an analysis increment method. The available analysis for the model is interpolated to the grid used for ECMWF data. The difference between interpolation and the new ECMWF analysis is an increment ("large scale increment") which is interpolated to the HIRLAM grid and added to get an updated HIRLAM analysis. Normal HIRLAM cycles then follow (03 UTC, 06 UTC, 09 UTC) in the morning to produce an "up-to-date" status of the atmosphere. In the evening the subsequent analyses are valid at 15 UTC, 18 UTC and 21 UTC, respectively. Using this method ATOVS data are implicitly used even if they are not assimilated into the HIRLAM model since ECMWF uses these data in their analysis system.

In order to compare the performance of different data assimilation experiments the

Figure 1: Daily bias- (lower, red) and rms-values (upper, green) for the 15 AMSU-A channels in the period January 26 to April 30, 2001.

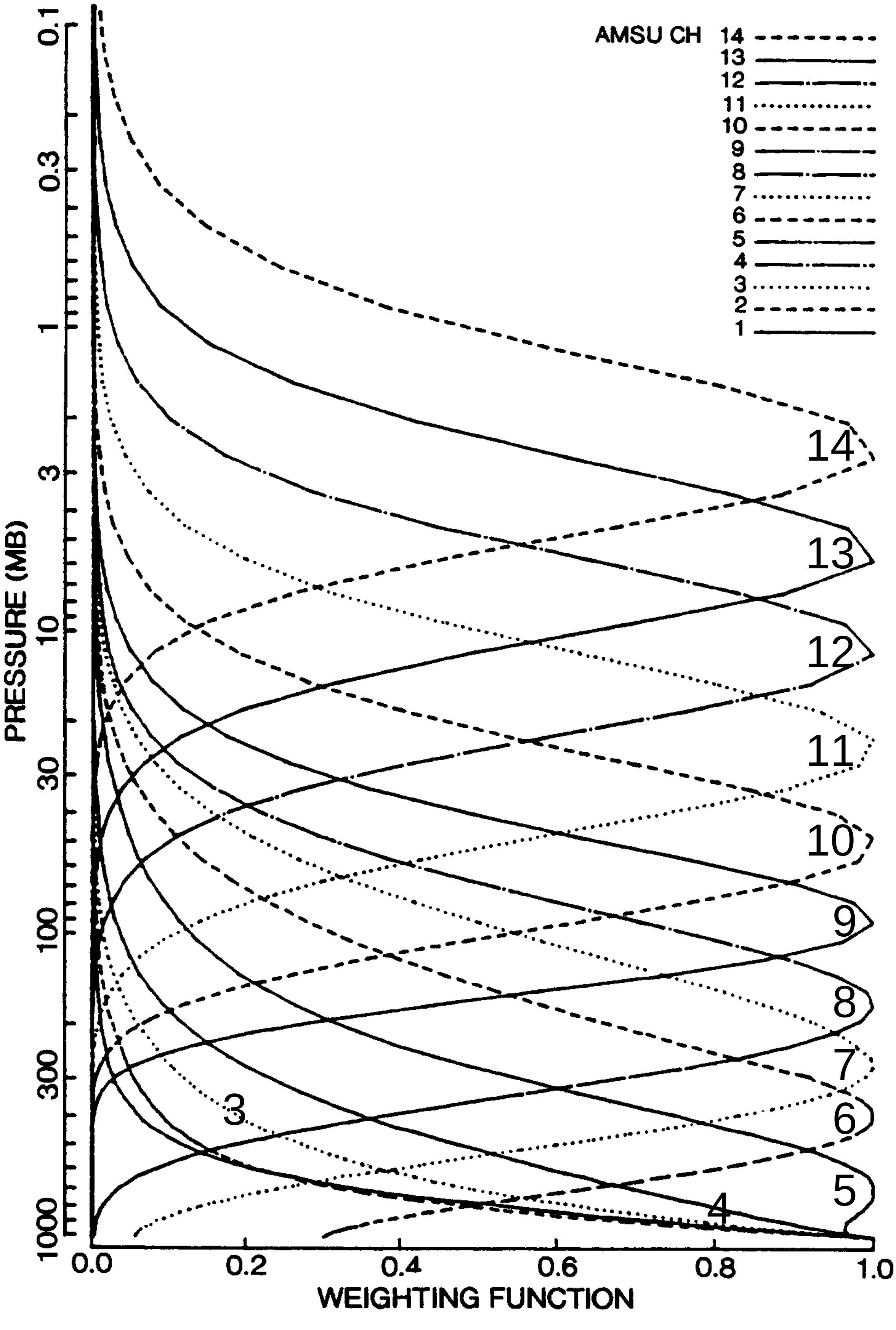

Figure 2: Normalized response/weighting functions for AMSU-A data. Each point corresponds to a data point. Figure taken from ECMWF notes for data assimilation course. (the notes are available under MET DA on `http://www.ecmwf.int/services/training/meteorology/index.html`)

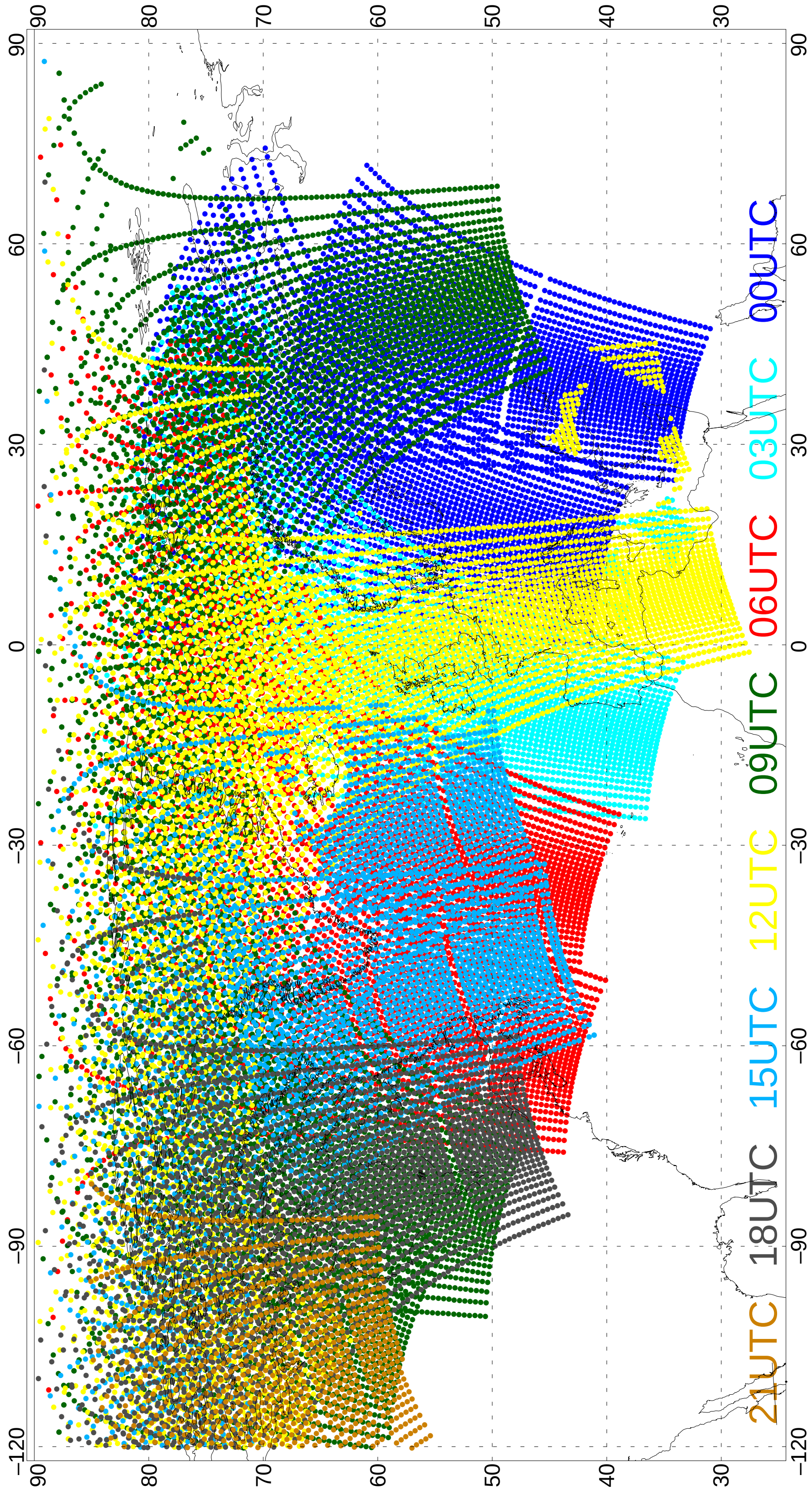

Figure 3: Data coverage for September 8 2001 of locally received ATOVS AMSU-A data. The data available for different assimilation cycles have different colors. The color is indicated at the bottom of the plot with the analysis time.

forecasts are verified against observations from European radiosonde and synoptic stations to give an objective evaluation of the experiments. Since the stations involved in this obs-verification cover a limited part of the model domain, the forecasts are also compared with initialized analyses from their own data assimilation suite (field-verification). The DMI observation- and field-verification packages are used.

The following "changes" have been made since the middle of July:

- Regularly update (every 7th to 14th day) of the bias correction file.
- Change of the observation error covariance matrix file ("dbt"-file), on July 19, based on data received from Smidsbjerg in March and April. Differences between first guess fields and observations were used.
- Change of the observation error covariance matrix file ("dbt"-file), on August 22, based on data received from Smidsbjerg and Sdr. Strømfjord in the period from July 20 to August 21. Differences between first guess fields and observations were used.
- Restart from the operational DMI-HIRLAM-G 00 UTC 3 and 6 hour forecasts on July 20.
- A convergence factor (epsg_qn) was changed from 0.05 to 0.01 if any AMSU-A data were available for the analysis except for the 00 UTC and 12 UTC runs.
- Since September 17 a new forecast model version with an update to the STRACO scheme and a change in the handling of ECMWF ice- and sst-fields has been used.

4. Results

For the first assimilation cycle the first guess (FG) fields were identical and a direct comparison of the statistics from the analyses can be made. Figure 4 shows the position of active NOAA16 data after data thinning from this data assimilation cycle and it is seen that they were in the Mediterranean Sea, the Black Sea, the Baltic Sea and the Barents Sea. The impact of these data on the analysis is illustrated in Figure 5 showing difference plots of the analyses for 850 hPa temperature and mean sea level pressure (mslp). As expected, the impact is largest close to the areas with AMSU-A data. Statistics for the FG and analysis for different observation types are illustrated in Table 3 and Figures 6 and 7. The results seems quite reasonable even though the SHIP and DRIBU statistics (Table 3) are somewhat better for NOA. It is also evident from Figure 7 that the channel 6 brightness temperature has the largest impact of the AMSU-A channels on the analysis.

After a period it was discovered that, except for the main synoptic hours 00 UTC and 12 UTC, the convergence criteria for stopping the iterations in the analysis were inadequate even when a limited number of AMSU-A data were included in the analysis. For the default convergence criteria the analysis often stopped after a few cycles and

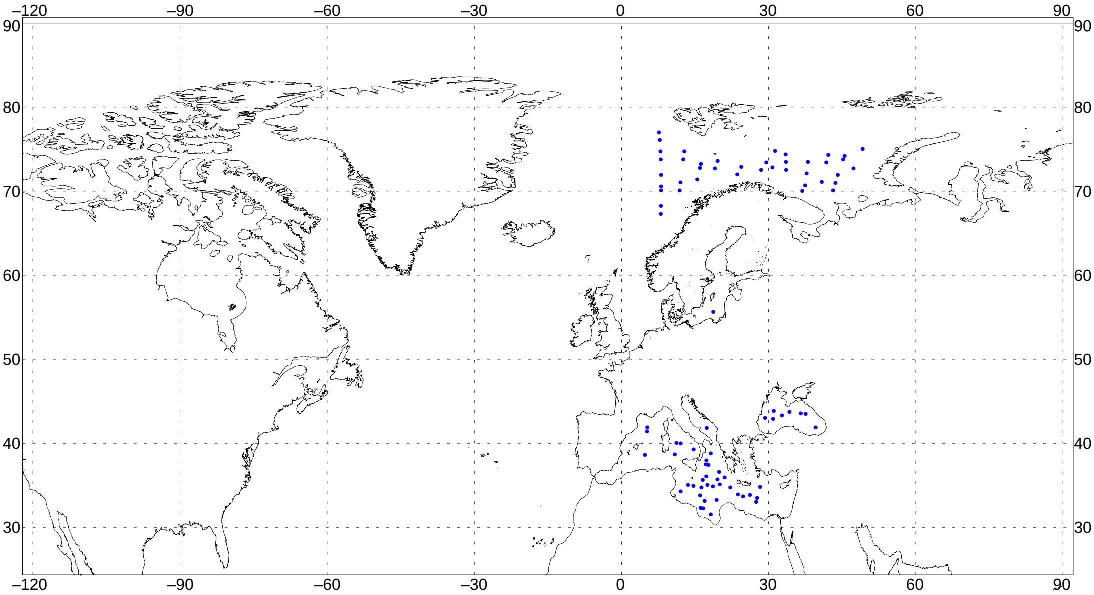

Figure 4: Positions (with blue dots) of active (after data thinning) NOAA16 data used in the analysis valid on 2001062500.

Table 3: Statistics for single level data. FG denotes the first guess statistics and "NOA" is the analysis statistics after the analysis without ATOVS. "WIA" denotes the analysis statistics with use of ATOVS.

		FG		NOA		WIA	
type	# obs.	bias	rms	bias	rms	bias	rms
SYNOP geop. ($m^2\,s^{-2}$)	1877	2.9	69.5	−0.9	41.7	−0.3	41.6
SHIP geop. ($m^2\,s^{-2}$)	258	1.7	93.4	4.8	55.2	2.7	76.6
DRIBU geop. ($m^2\,s^{-2}$)	58	−28.4	77.8	−14.0	43.8	−14.7	58.6

convergence was almost only for the brightness temperatures. This is illustrated for radiosonde data in Figure 8 for the analysis valid on 2001071206. Accordingly, one of the convergence criteria (the namelist variable `epsg_qn`) was changed and an example using the new value and a large number of active AMSU-A brightness temperatures is given in Figure 9 for the analysis valid on 2001080315. It is clear that a substantial part of the convergence is also for AIREP temperatures and wind, the rms-values are even lower for the WIA analysis including the brightness temperatures than for the NOA analysis.

Figure 10 shows values of the total cost functions (see Gustafsson *et al.*, 2001, or Mogensen *et al.*, 2000, for details on the cost function) from the 3D-Var analyses at 03 UTC and 15 UTC for the FG fields and the final analyses. Also the values for the total cost functions minus the AMSU-A part are given for WIA. It is evident that the FG values are very similar when the values for the model run WIA are reduced with the amount coming from the AMSU-A data. This is most probably caused by the restarts from ECMWF analyses at 00 UTC and 12 UTC in the assimilation schedule making the first guess fields almost the same at 03 UTC and 15 UTC.

4.1. Observation verification

Figures 11 and 12 show observation verification scores (bias and rms) for the July/August period (July 25, 00 UTC to August 31, 18 UTC) using the standard EWGLAM (European Working Group on Limited Area Modeling) station list. It is clear that the impact from using ATOVS brightness temperatures is very small for these parameters. However, there is a tendency towards WIA having marginally better rms-scores for long forecast lengths for upper level winds and 500 hPa temperature. The daily differences in the scores are also very small as can be seen for the August period in Figure 13. Figures 14 to 16 show similar plots for September 2001. For September the impact is very small, too, on these parameters. However, the tendency towards WIA having marginally better rms-scores for long forecast lengths for upper level winds and 500 hPa temperature is consistent.

4.2. Field verification

The field verifications showed very similar results for NOA and WIA with an overall neutral impact and accordingly no figure is included.

5. Conclusion

The OSE experiment has so far shown a basically neutral impact of including the AMSU-A brightness temperatures both overall and on a daily basis despite the differences in the resulting analyses. However, the impact in such a summer/early fall period is not expected to be large, especially not when restarting from ECMWF analyses twice a day. The runs should be continued to cover a full fall and a winter period.

The runs including AMSU-A brightness temperatures have been very stable and may be considered for real pre-operational testing as soon as a FG check has been implemented.

Acknowledgment

I would like to thank Kristian Mogensen for help in setting up the 3D-Var experiment and helpful discussions, Frank Tveter for helpful discussions and Tomas Landelius for providing the “dbt”-file used in the first part of the impact study.

References

Bouttier, F. and Kelly, G. 2001. Observing-system experiments in the ECMWF 4D-Var data assimilation system. *Quart. J. Roy. Meteorol. Soc.*, **127**, 1469–1488.

Gustafsson, N. and Svensson, J. 1988. A data assimilation experiment with high resolution TOVS data. *HIRLAM Technical Report*, **3**.

Gustafsson, N., Berre, L., Hörnquist, S., Huang, X.-Y., Lindskog, M., Navascués, B., Mogensen, K. S. and Thorsteinsson, S. 2001. Three-dimensional variational data assimilation for a limited area model. Part I: General formulation and the background error constraint. *Tellus*, **53A**, 425–446.

Gustafsson, Nils, Hörnquist, Sara, Lindskog, Magnus, Berre, Loïk, Navascués, Beatriz, Thorsteinsson, Sigurdur, Huang, Xiang-Yu, Mogensen, Kristian S. and Rantakokko, Jarmo. 1999. Three-dimensional variational data assimilation for a high resolution limited area model (HIRLAM). *HIRLAM Technical Report*, **40**.

Lindskog, M., Gustafsson, N., Navascués, B., Mogensen, K. S., Huang, X.-Y., Yang, X., Andræ, U., Berre, L., Thorsteinsson, S. and Rantakokko, J. 2001. Three-dimensional variational data assimilation for a limited area model. Part II: Observation handling and assimilation experiments. *Tellus*, **53A**, 447–468.

Mogensen, K. S., Jørgensen, Jess U., Amstrup, Bjarne, Yang, Xiaohua and Huang, Xiang-Yu. 2000. *Towards an operational implementation of HIRLAM 3D-VAR at DMI.* DMI Scientific Report 00-16. Danish Meteorological Institute.

Sass, Bent Hansen, Nielsen, Niels Woetmann, Jørgensen, Jess U., Amstrup, Bjarne and Kmit, Maryanne. 2000. *The Operational HIRLAM System at DMI - October 2000 -*. DMI Technical Report 00-26. Danish Meteorological Institute.

Saunders, R., Matricardi, M. and Brunel, P. 1999. An improved fast radiative transfer model for assimilation of satellite radiance observations. *Quart. J. Roy. Meteorol. Soc.*, **125**, 1407–1425.

Tveter, Frank Thomas and Vignes, Ole Nikolai. 2001. *Impact of ATOVS in HIRLAM 3D-VAR.* DNMI Research Note 55. Norwegian Meteorological Institute.

WMO. 1995. *Manual on codes, Volume I, International codes, Part B - Binary codes.* No 306, fm-94-ix, ext. bufr edn.

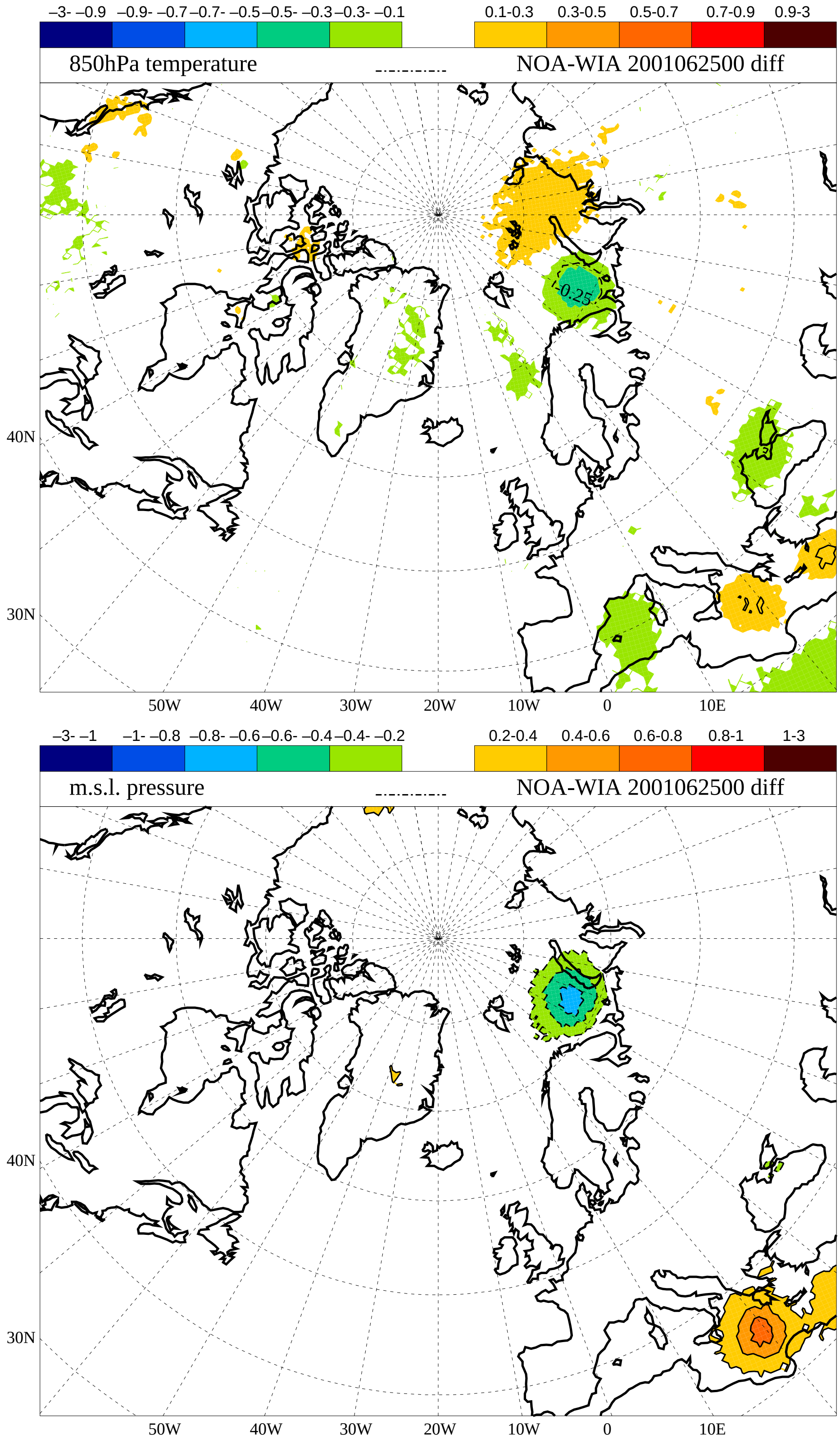

Figure 5: Difference plot of 850 hPa temperature (upper) and mslp (lower) of the analysis including AMSU-A brightness temperatures (WIA) and the analysis without AMSU-A brightness temperatures (NOA) valid on 20010625, 00 UTC. Contour lines are for every 0.25 K and 0.2 hPa, respectively.

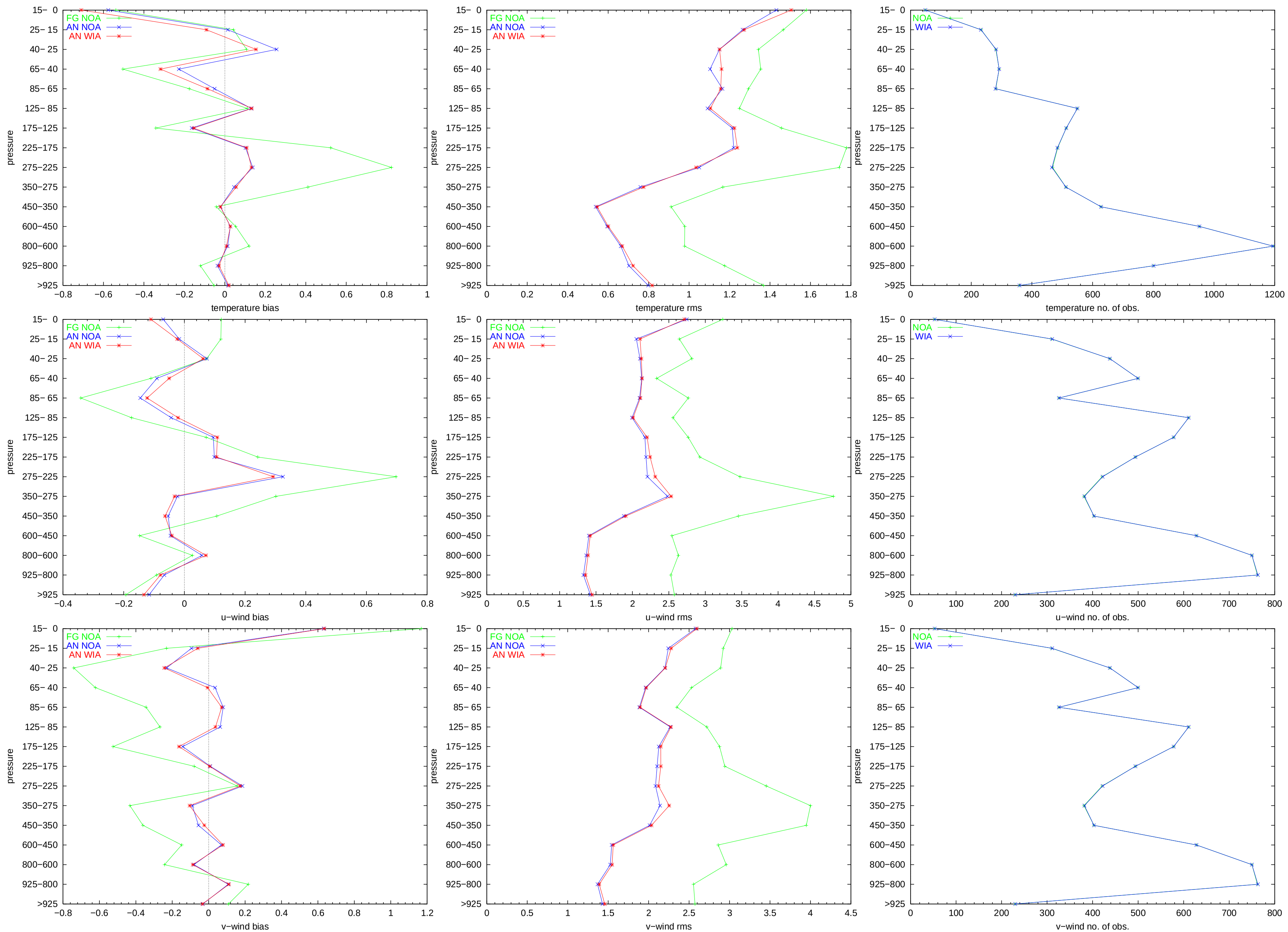

Figure 6: Statistical evaluation of the temperature, u-wind and v-wind radiosonde data in the 3D-Var analyses valid on 2001062500. NOA stands for the run without AMSU-A data and WIA stands for the run with AMSU-A data included. The first guess (denoted FG) rms and bias values are from the NOA analyses.

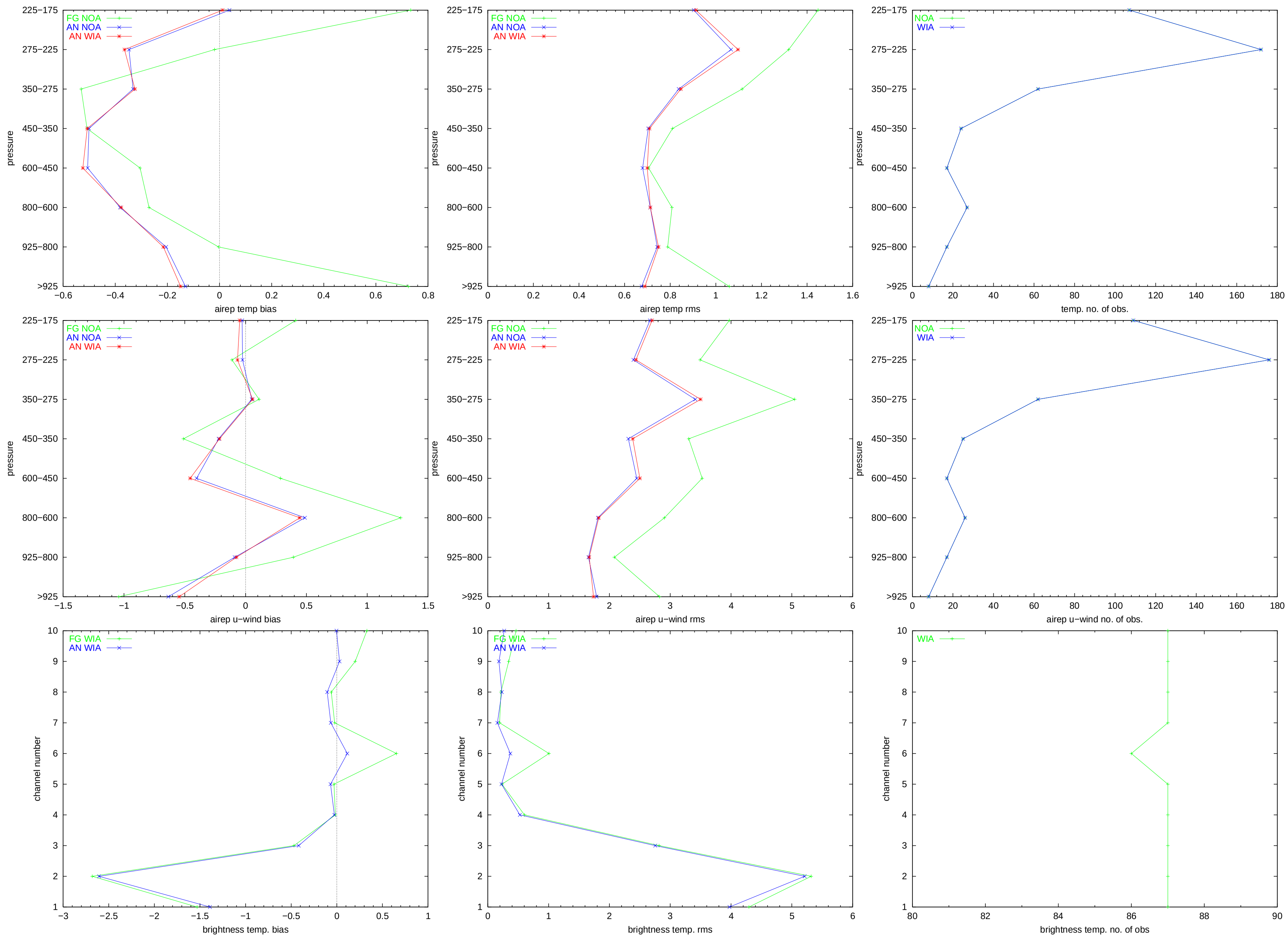

Figure 7: Statistical evaluation of AIREP temperature and u-wind data and brightness temperature data in the 3D-Var analyses valid on 2001062500. NOA stands for the run without AMSU-A data and WIA stands for the run with AMSU-A data included. The first guess (denoted FG) rms and bias values are for the analysis without AMSU-A data.

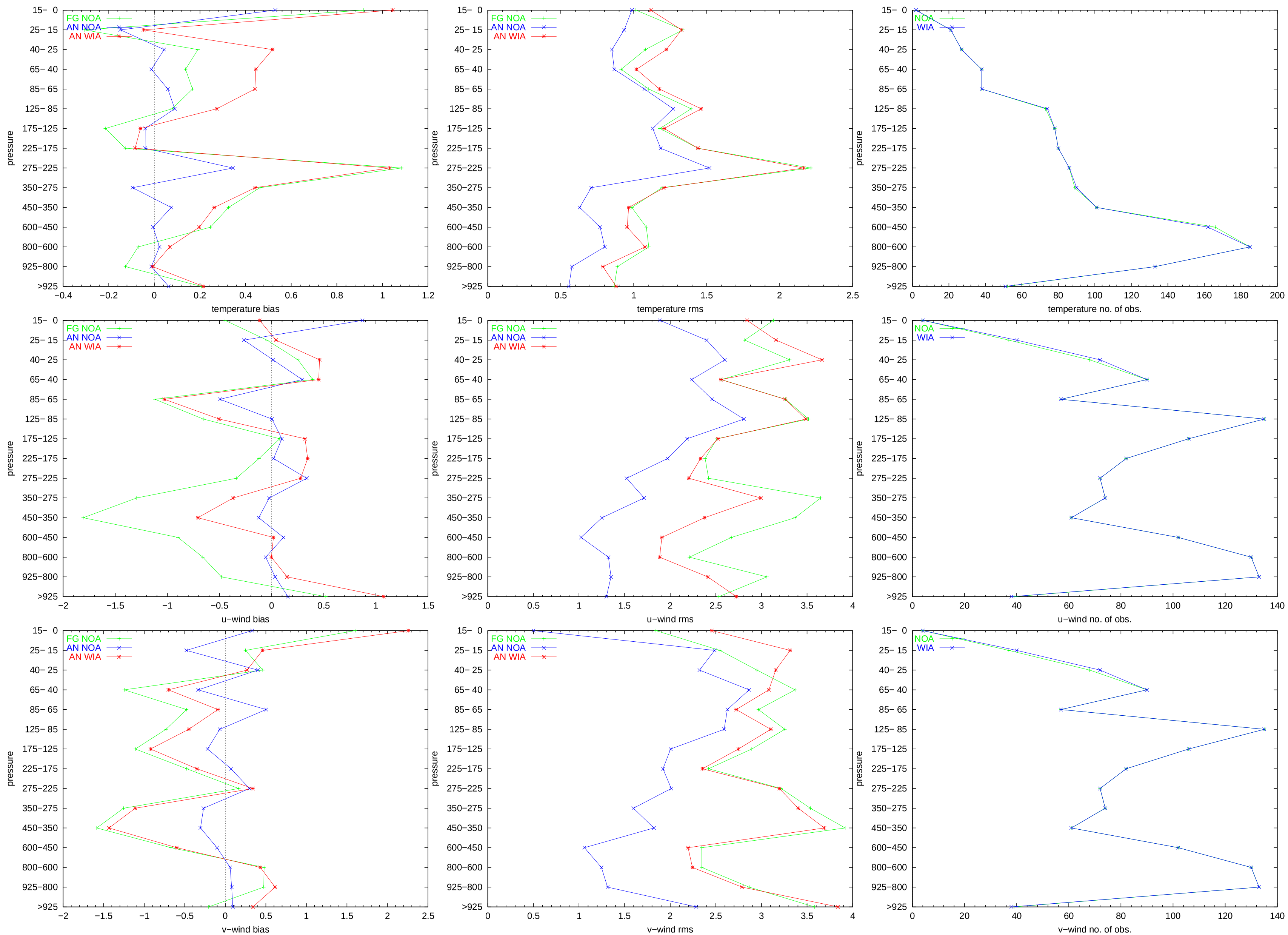

Figure 8: Statistical evaluation of the radiosonde data in the 3D-Var analyses valid on 2001071206. NOA stands for the run without AMSU-A data and WIA stands for the run with AMSU-A data included. The first guess (denoted FG) rms and bias values are for the analysis without AMSU-A data.

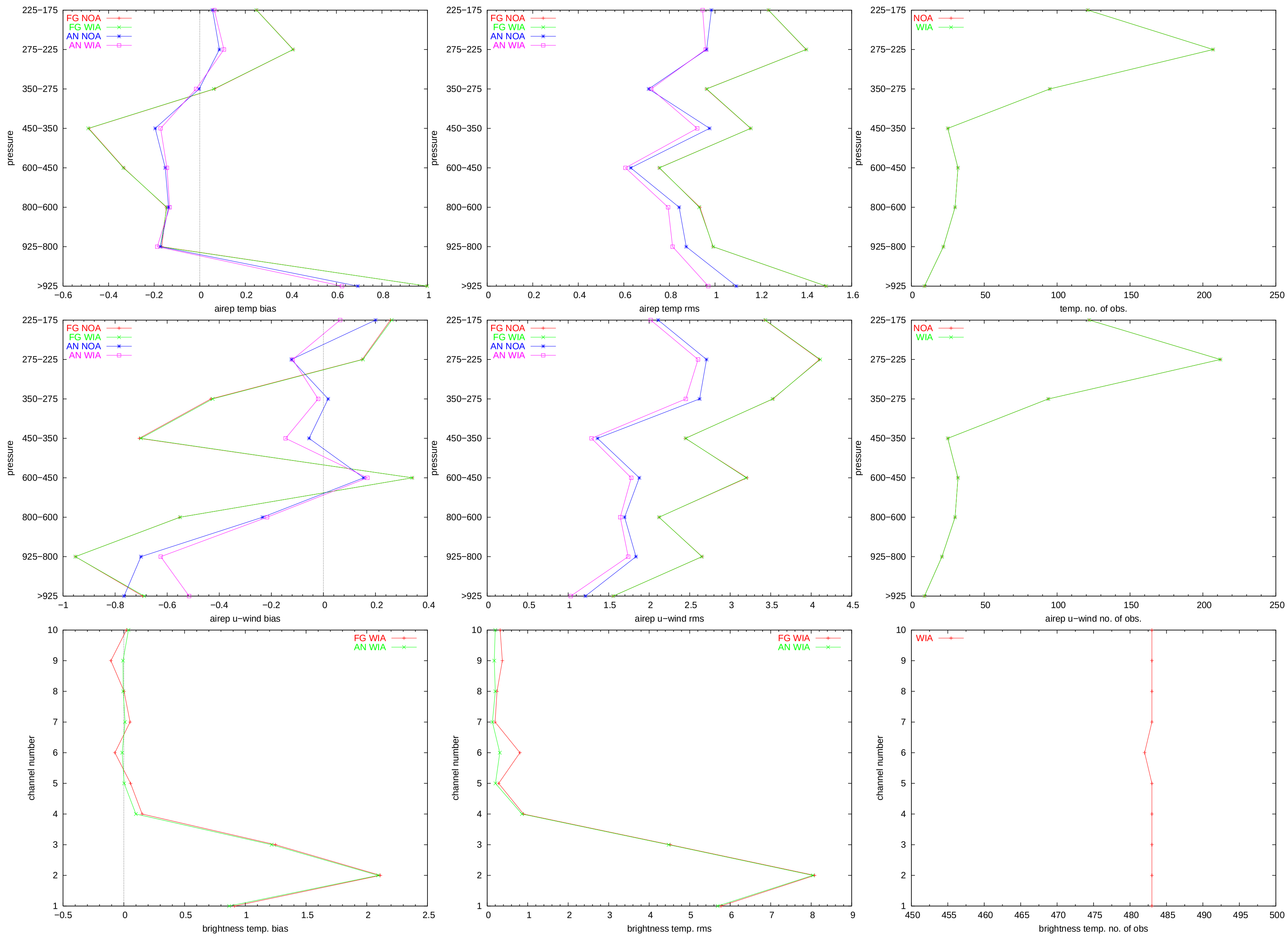

Figure 9: Statistical evaluation of AIREP temperature and u-wind data and brightness temperature data in the 3D-Var analyses valid on 2001080315. NOA stands for the run without AMSU-A data and WIA stands for the run with AMSU-A data included. The first guess (denoted FG) rms and bias values are for the analysis without AMSU-A data. The analyses are run with epsg_qn=0.01 (not 0.05). No radiosonde or pilots were available for these analyses.

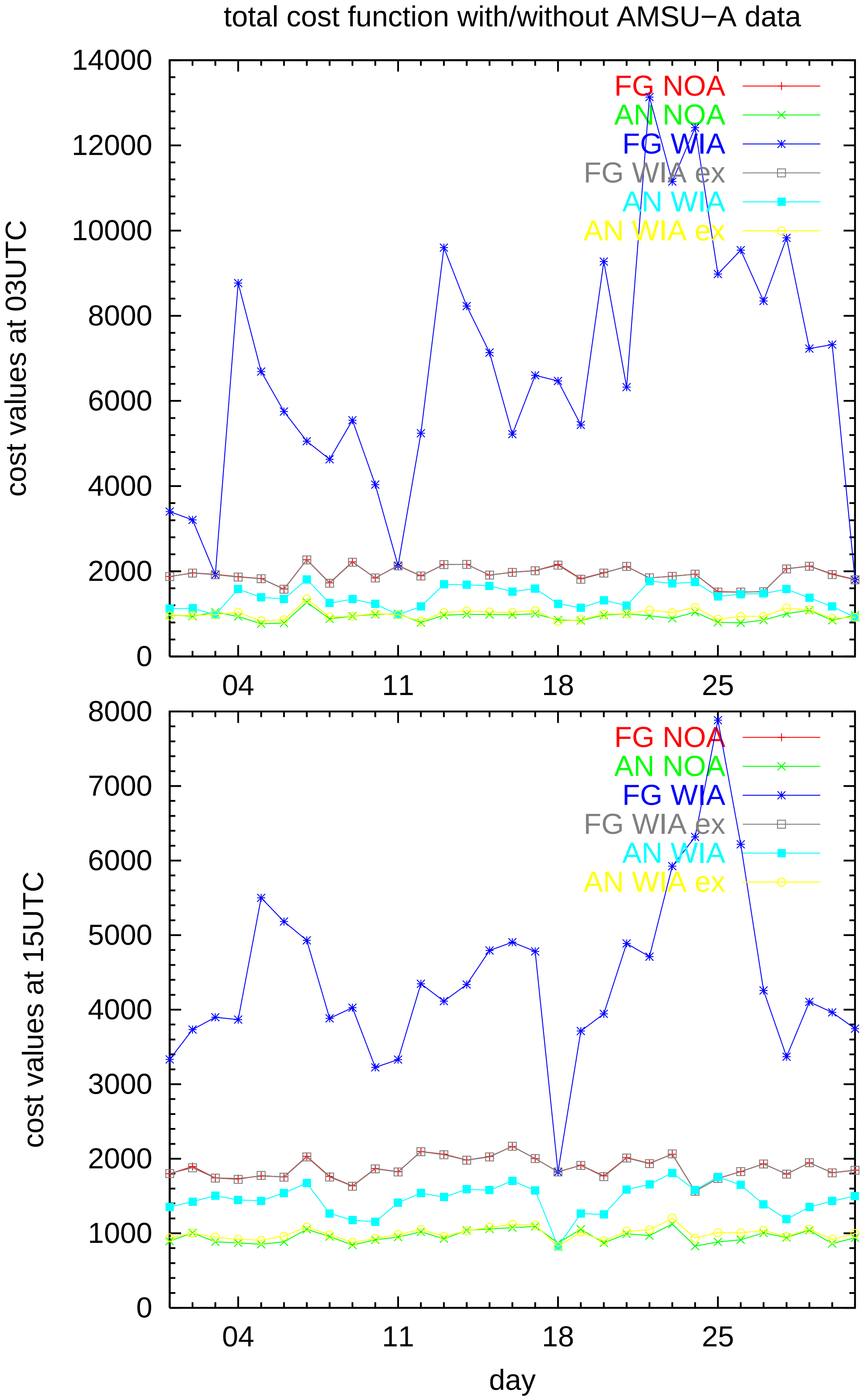

Figure 10: Cost function values for 03 UTC analyses and 15 UTC analyses in august. "FG NOA" stands for first guess values for the model run without inclusion of AMSU-A data and "AN NOA" is the same except but is the analysis value. Similarly "FG WIA" and "AN WIA" are for the run with inclusion of AMSU-A data. "FG WIA ex" and "AN WIA ex" are the total cost function for the model run with inclusion of AMSU-A data minus the AMSU-A part of cost function value. Note that "FG NOA" and "FG WIA ex" are very close in the plots.

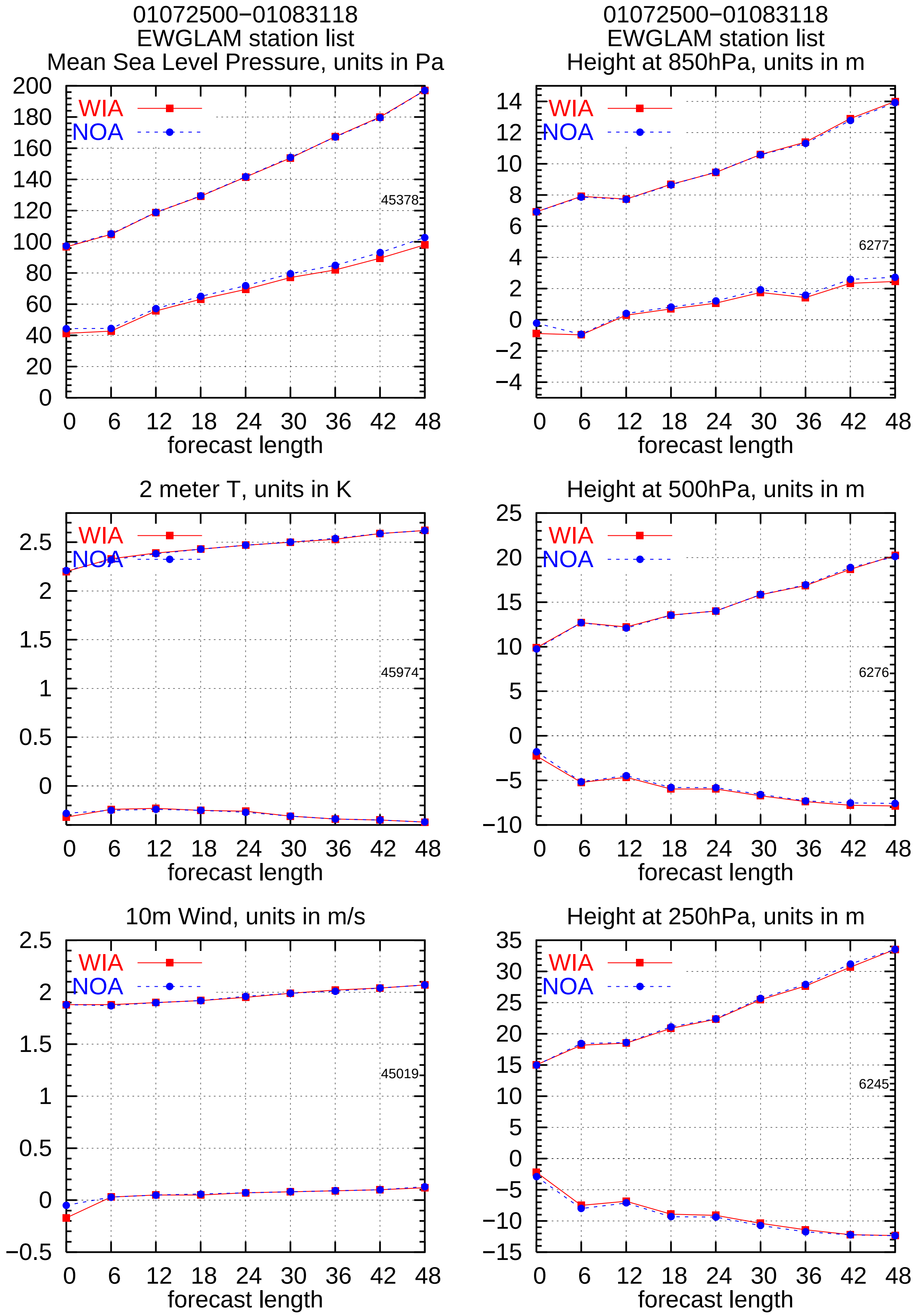

Figure 11: Obs-verification (bias and rms, EWGLAM station list) results for the July/August 2001 period of surface parameters and geopotential height for pressure levels specified in the plot. The small numbers in each plot indicate the number of observations used in the verification for the given variable.

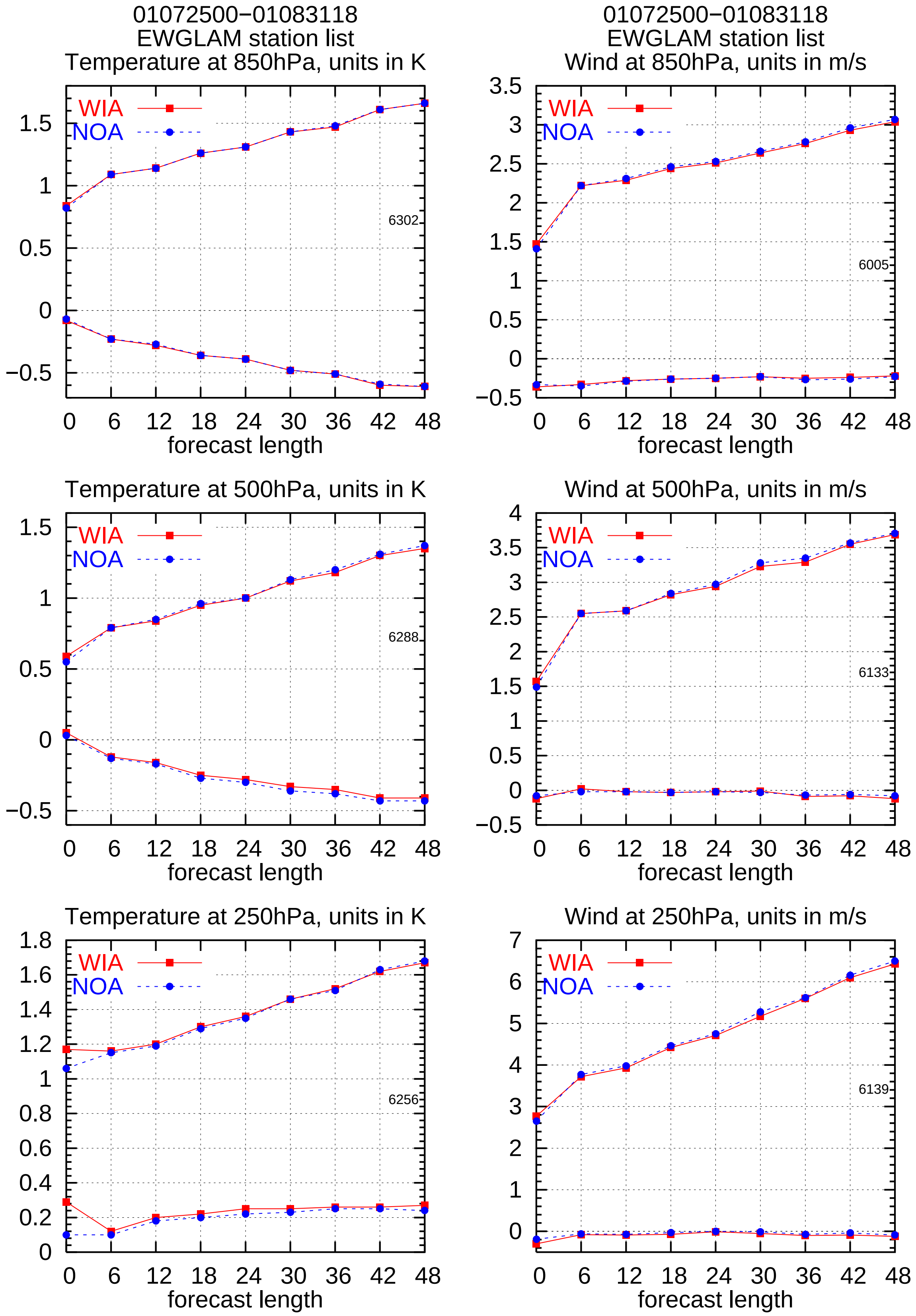

Figure 12: Obs-verification (bias and rms, EWGLAM station list) results for the July/August 2001 period of temperature and wind for pressure levels specified in the plot. The small numbers in each plot indicate the number of observations used in the verification for the given variable.

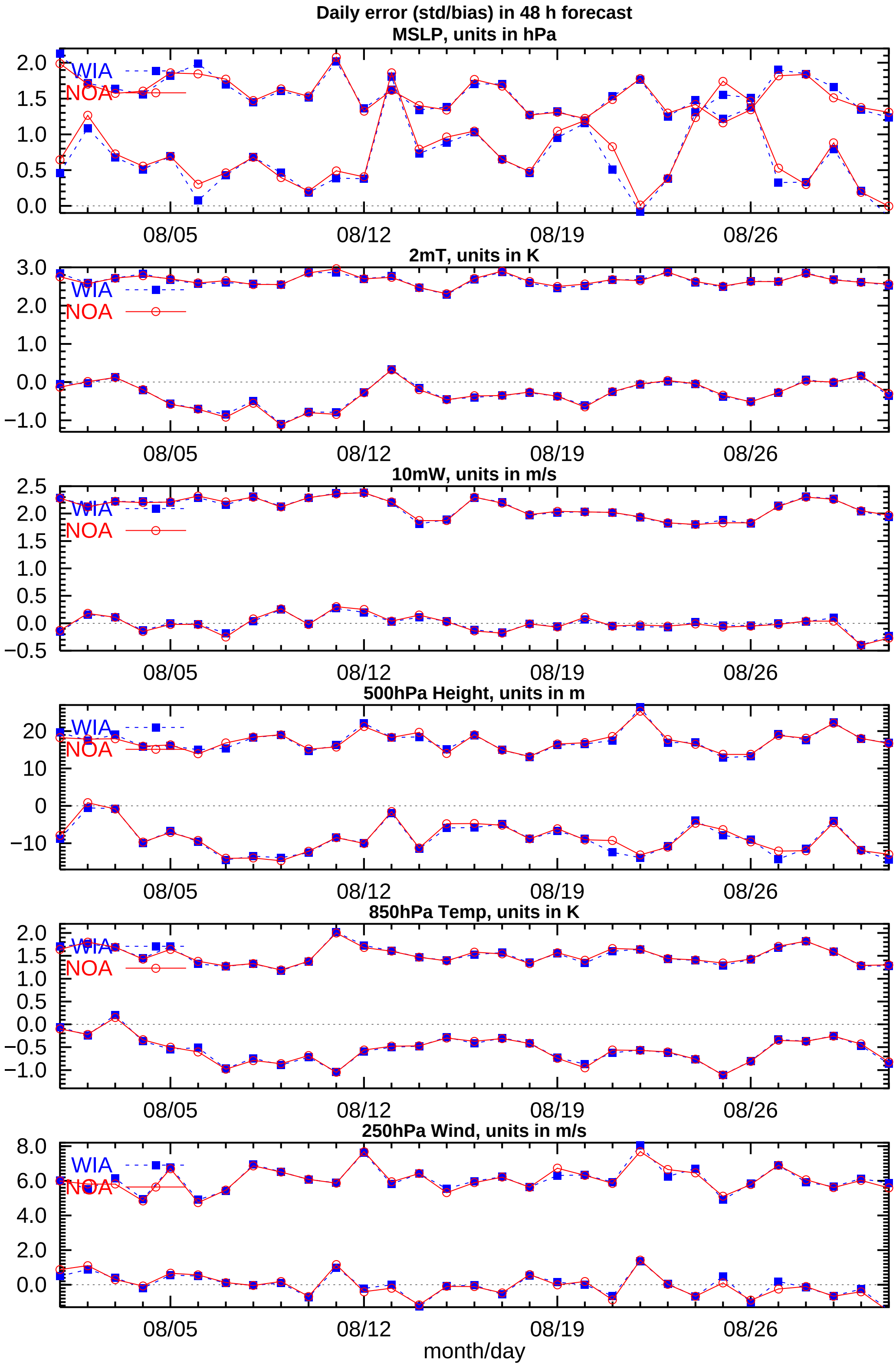

Figure 13: Daily obs-verification (bias and standard deviation, EWGLAM station list) results of 48 h forecasts for August 2001 of surface and upper level parameters specified in the plot.

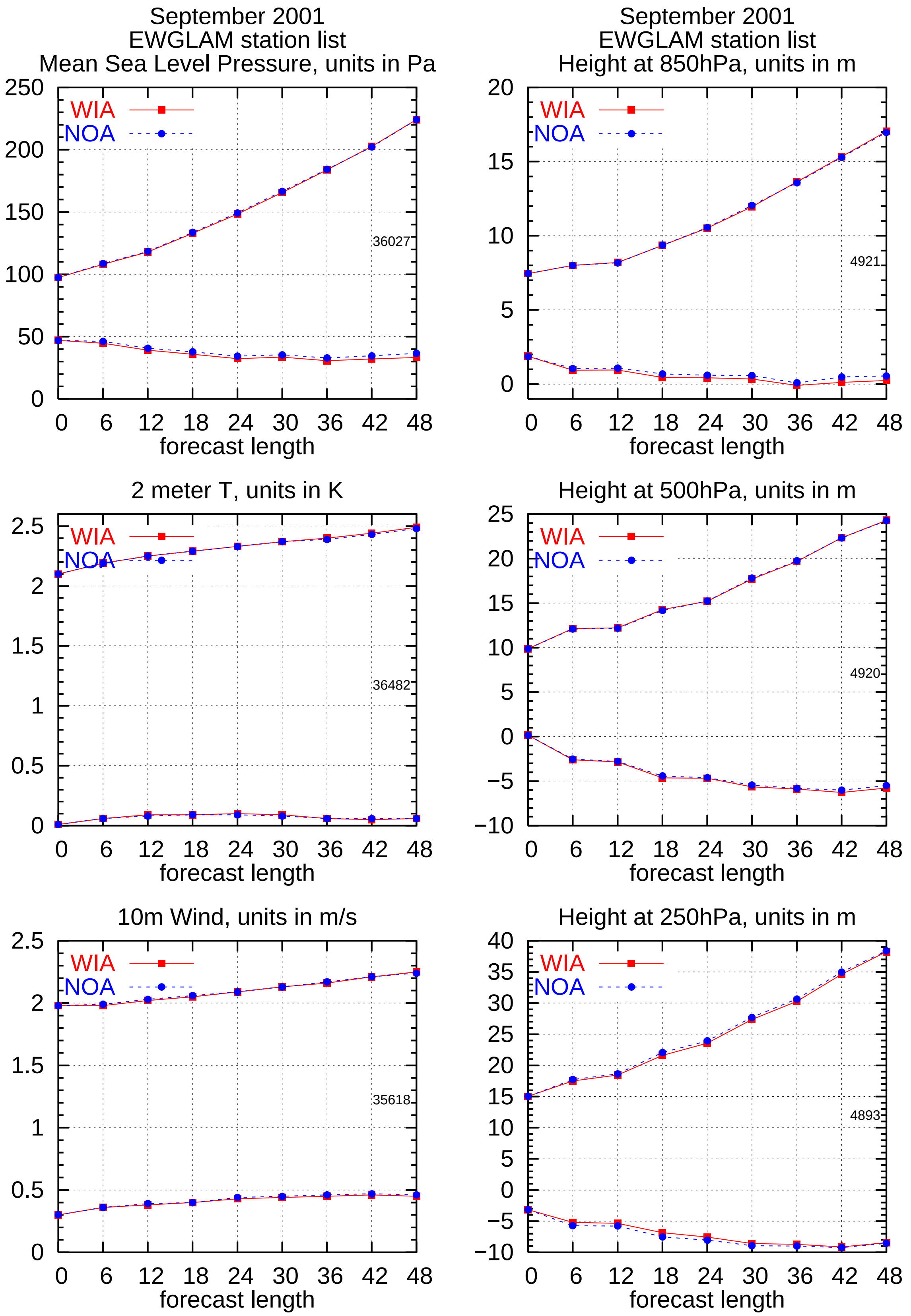

Figure 14: Obs-verification (bias and rms, EWGLAM station list) results for September 2001 of surface parameters and geopotential height for pressure levels specified in the plot. Operational DMI-HIRLAM-G analyses have been used to reject observations and the analysis verification scores are for the operational DMI-HIRLAM-G. The small numbers in each plot indicate the number of observations used in the verification for the given variable.

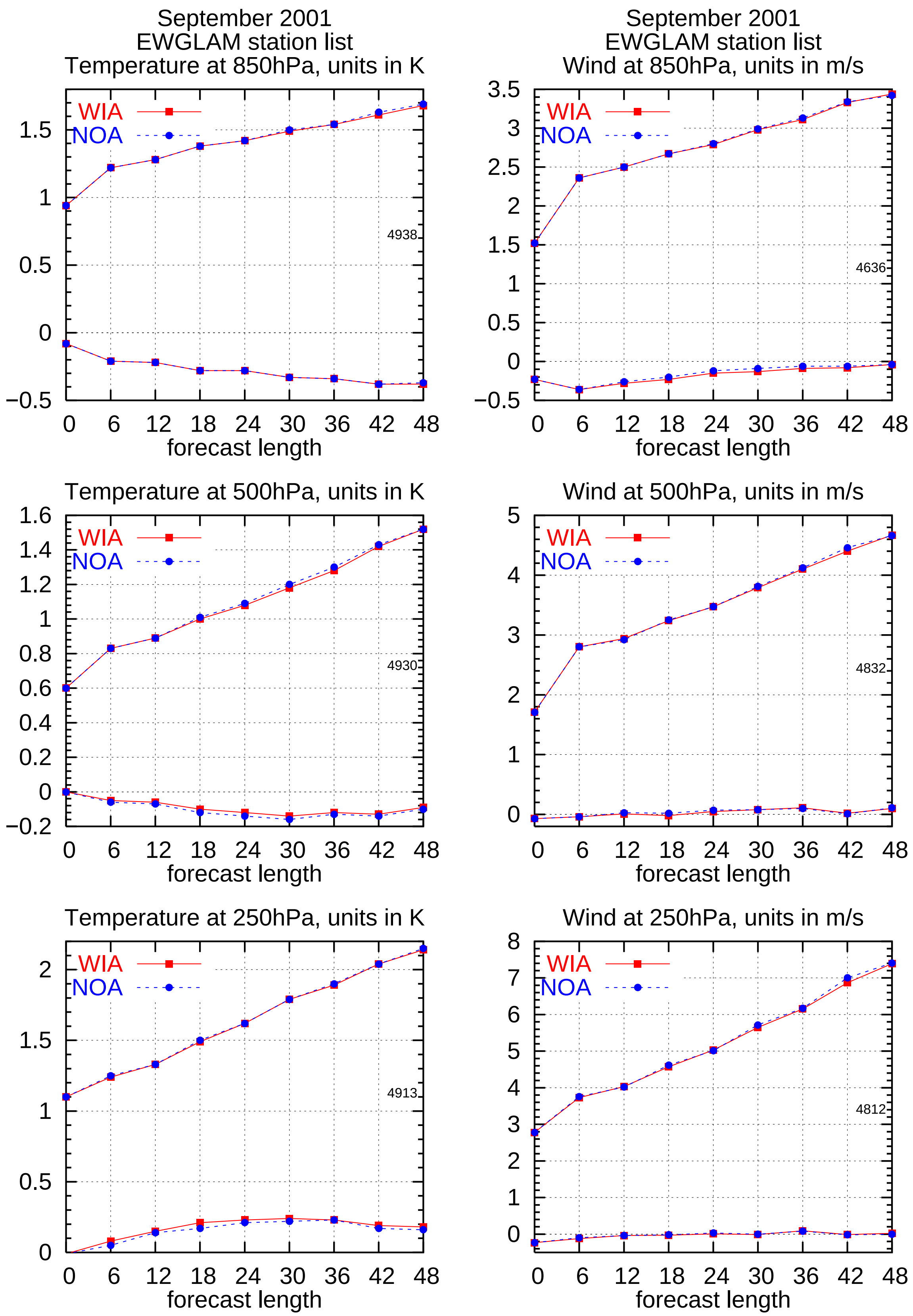

Figure 15: Obs-verification (bias and rms, EWGLAM station list) results for September 2001 of temperature and wind for pressure levels specified in the plot. Operational DMI-HIRLAM-G analyses have been used to reject observations and the analysis verification scores are for the operational DMI-HIRLAM-G. The small numbers in each plot indicate the number of observations used in the verification for the given variable.

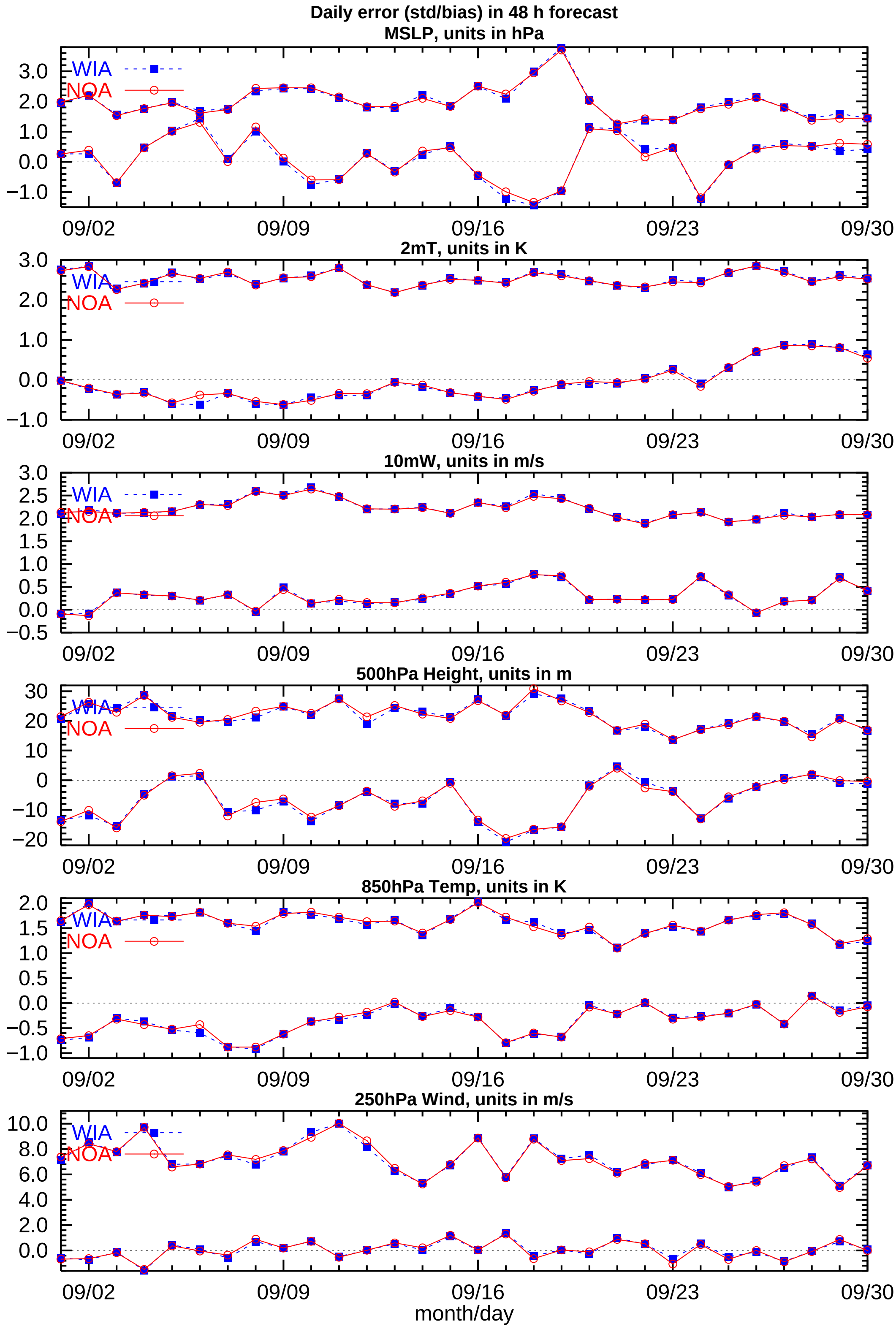

Figure 16: Daily obs-verification (bias and standard deviation, EWGLAM station list) results of 48 h forecasts for September 2001 of surface and upper level parameters specified in the plot.

DANISH METEOROLOGICAL INSTITUTE

Scientific Reports

Scientific reports from the Danish Meteorological Institute cover a variety of geophysical fields, i.e. meteorology (including climatology), oceanography, subjects on air and sea pollution, geomagnetism, solar-terrestrial physics, and physics of the middle and upper atmosphere.

Reports in the series within the last five years:

No. 96-1
Poul Frich (co-ordinator), H. Alexandersson, J. Ashcroft, B. Dahlström, G.R. Demarée, A. Drebs, A.F.V. van Engelen, E.J. Førland, I. Hanssen-Bauer, R. Heino, T. Jónsson, K. Jonasson, L. Keegan, P.Ø. Nordli, **T. Schmith**, **P. Steffensen**, H. Tuomenvirta, O.E. Tveito: North Atlantic Climatological Dataset (NACD Version 1) - Final report

No. 96-2
Georg Kjærgaard Andreasen: Daily response of high-latitude current systems to solar wind variations: application of robust multiple regression. Methods on Godhavn magnetometer data

No. 96-3
Jacob Woge Nielsen, Karsten Bolding Kristensen, Lonny Hansen: Extreme sea level highs: a statistical tide gauge data study

No. 96-4
Jens Hesselbjerg Christensen, Ole Bøssing Christensen, Philippe Lopez, Erik van Meijgaard, Michael Botzet: The HIRLAM4 Regional Atmospheric Climate Model

No. 96-5
Xiang-Yu Huang: Horizontal diffusion and filtering in a mesoscale numerical weather prediction model

No. 96-6
Henrik Svensmark and Eigil Friis-Christensen: Variation of cosmic ray flux and global cloud coverage - a missing link in solar-climate relationships

No. 96-7
Jens Havskov Sørensen and Christian Ødum Jensen: A computer system for the management of epidemiological data and prediction of risk and economic consequences during outbreaks of foot-and-mouth disease. CEC AIR Programme. Contract No. AIR3 - CT92-0652

No. 96-8
Jens Havskov Sørensen: Quasi-automatic of input for LINCOM and RIMPUFF, and output conversion. CEC AIR Programme. Contract No. AIR3 - CT92-0652

No. 96-9
Rashpal S. Gill and Hans H. Valeur: Evaluation of the radarsat imagery for the operational mapping of sea ice around Greenland

No. 96-10
Jens Hesselbjerg Christensen, Bennert Machenhauer, Richard G. Jones, Christoph Schär, Paolo Michele Ruti, Manuel Castro and Guido Visconti: Validation of present-day regional climate simulations over Europe: LAM simulations with observed boundary conditions

No. 96-11
Niels Larsen, Bjørn Knudsen, Paul Eriksen, Ib Steen Mikkelsen, Signe Bech Andersen and Torben Stockflet Jørgensen: European Stratospheric Monitoring Stations in the Artic: An European contribution to the Network for Detection of Stratospheric Change (NDSC): CEC Environment Programme Contract EV5V-CT93-0333: DMI contribution to the final report

No. 96-12
Niels Larsen: Effects of heterogeneous chemistry on the composition of the stratosphere: CEC Environment Programme Contract EV5V-CT93-0349: DMI contribution to the final report

No. 97-1
E. Friis Christensen og C. Skøtt: Contributions from the International Science Team. The Ørsted Mission - a pre-launch compendium

No. 97-2
Alix Rasmussen, Sissi Kiilsholm, Jens Havskov Sørensen, Ib Steen Mikkelsen: Analysis of tropospheric ozone measurements in Greenland: Contract No. EV5V-CT93-0318 (DG 12 DTEE): DMI's contribution to CEC Final Report Arctic Trophospheric Ozone Chemistry ARCTOC

No. 97-3
Peter Thejll: A search for effects of external events on terrestrial atmospheric pressure: cosmic rays

No. 97-4
Peter Thejll: A search for effects of external events on terrestrial atmospheric pressure: sector boundary crossings

No. 97-5
Knud Lassen: Twentieth century retreat of sea-ice in the Greenland Sea

No. 98-1
Niels Woetman Nielsen, Bjarne Amstrup, Jess U. Jørgensen:
HIRLAM 2.5 parallel tests at DMI: sensitivity to type of schemes for turbulence, moist processes and advection

No. 98-2
Per Høeg, Georg Bergeton Larsen, Hans-Henrik Benzon, Stig Syndergaard, Mette Dahl Mortensen: The GPSOS project
Algorithm functional design and analysis of ionosphere, stratosphere and troposphere observations

No. 98-3
Mette Dahl Mortensen, Per Høeg:
Satellite atmosphere profiling retrieval in a nonlinear troposphere
Previously entitled: Limitations induced by Multipath

No. 98-4
Mette Dahl Mortensen, Per Høeg:
Resolution properties in atmospheric profiling with GPS

No. 98-5
R.S. Gill and M. K. Rosengren
Evaluation of the Radarsat imagery for the operational mapping of sea ice around Greenland in 1997

No. 98-6
R.S. Gill, H.H. Valeur, P. Nielsen and K.Q. Hansen: Using ERS SAR images in the operational mapping of sea ice in the Greenland waters: final report for ESA-ESRIN's: pilot projekt no. PP2.PP2.DK2 and 2nd announcement of opportunity for the exploitation of ERS data projekt No. AO2..DK 102

No. 98-7
Per Høeg et al.: GPS Atmosphere profiling methods and error assessments

No. 98-8
H. Svensmark, N. Woetmann Nielsen and A.M. Sempreviva: Large scale soft and hard turbulent states of the atmosphere

No. 98-9
Philippe Lopez, Eigil Kaas and Annette Guldberg: The full particle-in-cell advection scheme in spherical geometry

No. 98-10
H. Svensmark: Influence of cosmic rays on earth's climate

No. 98-11
Peter Thejll and Henrik Svensmark: Notes on the method of normalized multivariate regression

No. 98-12
K. Lassen: Extent of sea ice in the Greenland Sea 1877-1997: an extension of DMI Scientific Report 97-5

No. 98-13
Niels Larsen, Alberto Adriani and Guido DiDonfrancesco: Microphysical analysis of polar stratospheric clouds observed by lidar at McMurdo, Antarctica

No.98-14
Mette Dahl Mortensen: The back-propagation method for inversion of radio occultation data

No. 98-15
Xiang-Yu Huang: Variational analysis using spatial filters

No. 99-1
Henrik Feddersen: Project on prediction of climate variations on seasonel to interannual timescales (PROVOST) EU contract ENVA4-CT95-0109: DMI contribution to the final report:Statistical analysis and post-processing of uncoupled PROVOST simulations

No. 99-2
Wilhelm May: A time-slice experiment with the ECHAM4 A-GCM at high resolution: the experimental design and the assessment of climate change as compared to a greenhouse gas experiment with ECHAM4/OPYC at low resolution

No. 99-3
Niels Larsen et al.: European stratospheric monitoring stations in the Artic II: CEC Environment and Climate Programme Contract ENV4-CT95-0136. DMI Contributions to the project

No. 99-4
Alexander Baklanov: Parameterisation of the deposition processes and radioactive decay: a review and some preliminary results with the DERMA model

No. 99-5
Mette Dahl Mortensen: Non-linear high resolution inversion of radio occultation data

No. 99-6
Stig Syndergaard: Retrieval analysis and methodologies in atmospheric limb sounding using the GNSS radio occultation technique

No. 99-7
Jun She, Jacob Woge Nielsen: Operational wave forecasts over the Baltic and North Sea

No. 99-8
Henrik Feddersen: Monthly temperature forecasts for Denmark - statistical or dynamical?

No. 99-9
P. Thejll, K. Lassen: Solar forcing of the Northern hemisphere air temperature: new data

No. 99-10
Torben Stockflet Jørgensen, Aksel Walløe Hansen: Comment on "Variation of cosmic ray flux and global coverage - a missing link in solar-climate relationships" by Henrik Svensmark and Eigil Friis-Christensen

No. 99-11
Mette Dahl Meincke: Inversion methods for atmospheric profiling with GPS occultations

No. 99-12
Hans-Henrik Benzon; Laust Olsen; Per Høeg: Simulations of current density measurements with a Faraday Current Meter and a magnetometer

No. 00-01
Per Høeg; G. Leppelmeier: ACE - Atmosphere Climate Experiment

No. 00-02
Per Høeg: FACE-IT: Field-Aligned Current Experiment in the Ionosphere and Thermosphere

No. 00-03
Allan Gross: Surface ozone and tropospheric chemistry with applications to regional air quality modeling. PhD thesis

No. 00-04
Henrik Vedel: Conversion of WGS84 geometric heights to NWP model HIRLAM geopotential heights

No. 00-05
Jérôme Chenevez: Advection experiments with DMI-Hirlam-Tracer

No. 00-06
Niels Larsen: Polar stratospheric clouds microphysical and optical models

No. 00-07
Alix Rasmussen: "Uncertainty of meteorological parameters from DMI-HIRLAM"

No. 00-08
A.L. Morozova: Solar activity and Earth's weather. Effect of the forced atmospheric transparency changes on the troposphere temperature profile studied with atmospheric models

No. 00-09
Niels Larsen, Bjørn M. Knudsen, Michael Gauss, Giovanni Pitari: Effects from high-speed civil traffic aircraft emissions on polar stratospheric clouds

No. 00-10
Søren Andersen: Evaluation of SSM/I sea ice algorithms for use in the SAF on ocean and sea ice, July 2000

No. 00-11
Claus Petersen, Niels Woetmann Nielsen: Diagnosis of visibility in DMI-HIRLAM

No. 00-12
Erik Buch: A monograph on the physical oceanography of the Greenland waters

No. 00-13
M. Steffensen: Stability indices as indicators of lightning and thunder

No. 00-14
Bjarne Amstrup, Kristian S. Mogensen, Xiang-Yu Huang: Use of GPS observations in an optimum interpolation based data assimilation system

No. 00-15
Mads Hvid Nielsen: Dynamisk beskrivelse og hydrografisk klassifikation af den jyske kyststrøm

No. 00-16
Kristian S. Mogensen, Jess U. Jørgensen, Bjarne Amstrup, Xiaohua Yang and Xiang-Yu Huang: Towards an operational implementation of HIRLAM 3D-VAR at DMI

No. 00-17
Sattler, Kai; Huang, Xiang-Yu: Structure function characteristics for 2 meter temperature and relative humidity in different horizontal resolutions

No. 00-18
Niels Larsen, Ib Steen Mikkelsen, Bjørn M. Knudsen m.fl.: In-situ analysis of aerosols and gases in the polar stratosphere. A contribution to THESEO. Environment and climate research programme. Contract no. ENV4-CT97-0523. Final report

No. 00-19
Amstrup, Bjarne: EUCOS observing system experiments with the DMI HIRLAM optimum interpolation analysis and forecasting system

No. 01-01
V.O. Papitashvili, L.I. Gromova, V.A. Popov and O. Rasmussen: Northern polar cap magnetic activity index PCN: Effective area, universal time, seasonal, and solar cycle variations

No. 01-02
M.E. Gorbunov: Radioholographic methods for processing radio occultation data in multipath regions

No. 01-03
Niels Woetmann Nielsen; Claus Petersen: Calculation of wind gusts in DMI-HIRLAM

No. 01-04
Vladimir Penenko; Alexander Baklanov: Methods of sensitivity theory and inverse modeling for estimation of source parameter and risk/vulnerability areas

No. 01-05
Sergej Zilitinkevich; Alexander Baklanov; Jutta Rost; Ann-Sofi Smedman, Vasiliy Lykosov and Pierluigi Calanca: Diagnostic and prognostic equations for the depth of the stably stratified Ekman boundary layer